Proceedings of the Estonian Academy of Sciences,
2019, **68**, 1, 111–123
https://doi.org/10.3176/proc.2019.1.11
Available online at www.eap.ee/proceedings

COMMUNICATIONS
TECHNOLOGY

Energy harvesting based two-way full-duplex relaying network over a Rician fading environment: performance analysis

Tan N. Nguyen[a,b], Minh Tran[c*], Duy-Hung Ha[b,d], Thanh-Long Nguyen[e], and Miroslav Voznak[b]

[a] Wireless Communications Research Group, Faculty of Electrical and Electronics Engineering, Ton Duc Thang University, Ho Chi Minh City, Vietnam
[b] VSB-Technical University of Ostrava, 17. listopadu 15/2172, 708 33 Ostrava - Poruba, Czech Republic
[c] Optoelectronics Research Group, Faculty of Electrical and Electronics Engineering, Ton Duc Thang University, Ho Chi Minh City, Vietnam
[d] Faculty of Electrical and Electronics Engineering, Ton Duc Thang University, Ho Chi Minh City, Vietnam
[e] Center for Information Technology, Ho Chi Minh City University of Food Industry, Ho Chi Minh City, Vietnam

Received 12 June 2018, accepted 2 October 2018, available online 21 February 2019

Abstract. Full-duplex transmission is a promising technique to enhance the capacity of communication systems. In this paper, we propose and investigate the system performance of an energy harvesting based two-way full-duplex relaying network over a Rician fading environment. Firstly, we analyse and demonstrate the analytical expressions of the achievable throughput, outage probability, optimal time switching factor, and symbol error ratio of the proposed system. In the second step, the effect of various parameters of the system on its performance is presented and investigated. In the final step, the analytical results are also demonstrated by Monte Carlo simulation. The numerical results proved that the analytical results and the simulation results agreed with each other.

Key words: full duplex, throughput, outage probability, wireless energy harvesting, symbol error ratio.

1. INTRODUCTION

Relay communication, in which the relay forwards the signal received by a source to a destination, has a huge consideration in research due to its ability to expand the coverage, increase the capacity, and reduce the power consumption [1–4]. Moreover, relaying the communication network is an effective way to combat the performance degradation caused by fading, shadowing, or path loss and is an efficient way to improve spectrum efficiency and extend coverage. In the first step, the relay node operates in the half-duplex (HD) mode, in which the node transmits and receives signals in the orthogonal frequency or time resources. In order to satisfy the increasing data rate demands, the research in the fifth generation (5G) wireless networks is ongoing, both in academia and industry. In the 5G era, wireless networks should offer up to tens of Gbps data rate to support a variety of emerging services, which stimulates researchers to explore innovative techniques continually, with higher spectrum efficiency.

* Corresponding author, tranhoangquangminh@tdtu.edu.vn

The concept of the full-duplex (FD) technique, which allows the communication node to transmit and receive signals over the same frequency band at the same time slot, has been proposed and discussed [1–6]. In comparison with the HD mode, the FD mode can double the spectral efficiency, because it exploits the resources more efficiently. An FD scheme, where the transmission and the reception are at the same time on the same channel, achieves up to double the capacity of an HD scheme. Two-way relaying, where two users exchange information with each other via a single relay or multiple relays, provides improved spectral efficiency compared to conventional one-way relaying by using either superposition coding or physical layer network coding at relays. Furthermore, to satisfy the 5G requirements, relaying schemes with high spectrum efficiency, such as two-way, full-duplex, etc., have recently attracted considerable attention. Relaying and FD schemes are combined to achieve higher data rates [7–10].

In [7], the authors investigate one-way full-duplex (OWFD) relaying and two-way half-duplex (TWHD) relaying to minimize/recover the spectral efficiency loss associated with OWHD relaying, which requires additional resources (e.g. time slots or frequencies) to transmit data. In [8] and [9], the authors present OWFD relaying with multiple antennas to provide a solution to overcome the spectral efficiency loss in OWHD relaying. In [10], the authors investigate OWFD relaying with an opportunistic relay selection to enhance the performance of OWHD relaying. Most previous studies are focused on OWFD relaying, and there have been few works on TWFD relaying.

In this paper, the system performance of the energy harvesting based TWFD relaying network over a Rician fading environment is proposed and investigated. Firstly, we analyse and demonstrate the analytical expressions of the achievable throughput, outage probability, optimal time switching factor, and symbol error ratio (SER) of the proposed system. In the second step, the effect of various parameters of the system on its performance is presented and investigated. In the final step, the analytical results are also demonstrated by Monte Carlo simulation. The numerical results demonstrated that the analytical results and the simulation results agreed with each other. The main contributions of the paper are summarized as follows:

- The system model of energy harvesting based TWFD relaying network over a Rician fading environment with the time switching protocol is proposed and investigated.
- The closed form of the outage probability and throughput of the proposed system is derived.
- The influence of the main parameters on the system performance is demonstrated.
- The optimal time switching factor and SER are investigated and calculated in connection with the main system parameters.

The remainder of this paper is organized as follows. Section 2 presents the system model of the model system. Section 3 proposes and demonstrates the analytical mathematical expressions of the outage probability, throughput, the optimal time switching factor, and the SER of the system. Section 4 provides the numerical results and some discussions. Section 5 concludes the paper. Finally, the appendices present the proofs of the theorems.

2. SYSTEM MODEL

In this section, an energy harvesting based TWFD relaying network over a Rician fading environment is proposed. Figure 1 illustrates the information transmission and energy transfer between the nodes A and B via the helping relay R. In this system model, both nodes A and B have two antennas, one of which is responsible for signal transmission and the other for signal reception. The line topology is adopted, where the relay node is located on the straight line connecting the two source nodes. Assume that the two source nodes cannot receive signals from each other directly due to the high path loss caused by obstacles [5–7]. In this model, the following two assumptions are considered:

- There is no connection between the source and the destination in the results of elimination transmission information.
- The required power of the data decoding process at the relay is negligible in comparison to the signal transmission energy from the relay to the destination.

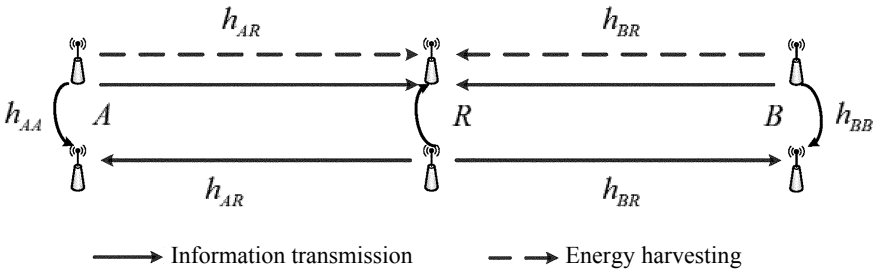

Fig. 1. System model.

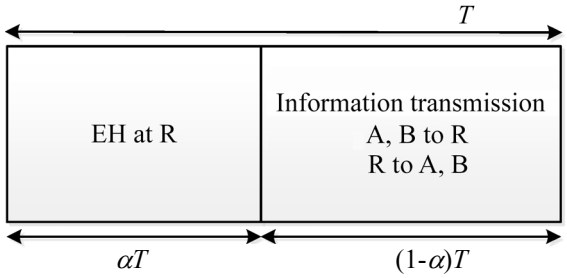

Fig. 2. Energy harvesting (EH) and information processing.

Moreover, the energy harvesting and information processing at the relay by the time switching protocol are shown in Fig. 2, where T is the block time in which the nodes A and B are connected with each other via the helping relay R. In this model, the first interval time αT is used for energy harvesting at the relay R from the nodes A and B. After that, the information transmission process between the nodes A and B via the helping relay R is done in the remaining interval time $(1\text{-}\alpha)T$, $\alpha \in (0, 1)$.

3. SYSTEM PERFORMANCE

In this section, the outage probability, achievable throughput, optimal time switching factor, and SER are investigated.

The total harvested energy of R during energy harvesting time αT is given by (1):

$$E_R = \eta P_{AB}\left(\left|h_{AR}\right|^2 + \left|h_{BR}\right|^2\right)\alpha T, \tag{1}$$

where $0 < \eta < 1$ is the energy conversion efficiency, which depends on the rectification process and the energy harvesting circuitry [11], and $P_A = P_B = P_{AB}$ denotes the transmission power of the nodes A and B.

The average transmission power of R is computed by (2):

$$P_R = \frac{E_R}{(1-\alpha)T} = \frac{\eta\alpha T P_{AB}}{(1-\alpha)T}\left(\left|h_{AR}\right|^2 + \left|h_{BR}\right|^2\right) = \kappa P_{AB}\left(\left|h_{AR}\right|^2 + \left|h_{BR}\right|^2\right), \tag{2}$$

where we denote $\kappa = \dfrac{\eta\alpha}{1-\alpha}$.

Due to the FD system, the multiple-access phase (MAP) and the broadcast phase (BCP) can work at the same time. Therefore, the received signal at the relay can be expressed as (3):

$$y_R = h_{AR}x_A + h_{BR}x_B + h_{RR}x_R + n_R, \tag{3}$$

where x_A, x_B denote the transmission signal from A and B, respectively, h_{RR} is the residual self-interference channel at R, and n_R is the zero-mean additive white Gaussian noise (AWGN) with variance N_0,

$$\mathrm{E}\left\{\left|x_A\right|^2\right\} = \mathrm{E}\left\{\left|x_B\right|^2\right\} = P_{AB};\ \mathrm{E}\left\{\left|x_R\right|^2\right\} = P_R,$$

where E{.} denotes the expectation operation and h_{AR}, h_{BR} are the Rician distribution factors.

In the research model, the amplify-and-forward (AF) protocol is used. Hence, the received signal at the relay R is amplified by a factor β, which is given by the following:

$$\beta = \frac{x_R}{y_R} = \sqrt{\frac{P_R}{P_{AB}\left|h_{AR}\right|^2 + P_{AB}\left|h_{BR}\right|^2 + P_R\left|h_{RR}\right|^2 + N_0}}. \tag{4}$$

Then the received signal at the node A can be expressed as:

$$y_A = h_{AR}x_R + h_{AA}x_A + n_A, \tag{5}$$

where x_R is the transmission signal from R, h_{AA} denotes the residual self-interference channel at the node A, and n_A is the AWGN with variance N_0.

Combine (3) and (4), then (5) can be rewritten as:

$$\begin{aligned} y_A &= h_{AR}\beta y_R + h_{AA}x_A + n_A = h_{AR}\beta\left[h_{AR}x_A + h_{BR}x_B + h_{RR}x_R + n_R\right] + h_{AA}x_A + n_A \\ &= \beta h_{AR}^2 x_A + \beta h_{AR}h_{BR}x_B + \beta h_{AR}h_{RR}x_R + \beta h_{AR}n_R + h_{AA}x_A + n_A. \end{aligned} \tag{6}$$

In equation (6), the first term of the equation ($\beta h_{AR}^2 x_A$) can be removed due to the network coding as presented in [12]. By substituting (2) and (4) into (6), with some mathematical manipulation, the received signal to interference noise ratio (SINR) at the node A can be obtained as:

$$\gamma_A = \frac{\kappa\psi^2\left|h_{AR}\right|^2\left|h_{BR}\right|^2\left(\left|h_{AR}\right|^2 + \left|h_{BR}\right|^2\right)}{\left[\left(\left|h_{AR}\right|^2 + \left|h_{BR}\right|^2\right)\psi\left(\kappa\left|h_{AR}\right|^2 N_0 + N_0\right)\right] + 1}, \tag{7}$$

where we denote $\psi = \dfrac{P_{AB}}{\Omega_{RR}+1} = \dfrac{P_{AB}}{\Omega_{AA}+1}$.

In the high SINR region, (7) can be approximated as follows:

$$\gamma_A \approx \frac{\kappa\psi XY}{\kappa XN_0 + N_0} = \frac{\kappa\varphi\omega_1\omega_2}{\kappa\omega_1 + 1}, \tag{8}$$

where we denote $\varphi = \dfrac{\psi}{N_0}, \omega_1 = \left|h_{AR}\right|^2, \omega_2 = \left|h_{BR}\right|^2$.

In this analysis, please note that for convenience, the residual self-interference at the three nodes is modelled as AWGN with zero mean and variance of $\Omega_{RR}, \Omega_{AA}, \Omega_{BB}$, which are identical [13]. In addition, please note that if we set $\Omega = \Omega_{RR} = \Omega_{AA} = \Omega_{BB} = 0$ and $\kappa = \dfrac{2\eta\alpha}{1-\alpha}$ [4], γ_A turn into SINR of the HD AF relay system.

For similarity, we can obtain SINR at the node B as:

$$\gamma_B = \frac{\kappa\varphi\omega_1\omega_2}{\kappa\omega_2 + 1}. \tag{9}$$

3.1. Outage probability

In this work, we consider the delay limited transmission mode, where the average throughput can be computed from the outage probability.

Theorem 1. *The outage probability at the source nodes A and B can be computed by equations* (10):

$$\begin{aligned} P_{out\_A} &= 1 - 2a_1a_2 \times e^{-\frac{b_2\gamma_{th}}{\varphi}} \sum_{l=0}^{\infty}\sum_{k=0}^{\infty}\sum_{m=0}^{l}\sum_{n=0}^{m} \frac{K^{l+k} b_1^{\frac{k+n-1}{2}} b_2^{\frac{2m+k-n-1}{2}}}{l!n!(m-n)!(k!)^2 \kappa^{\frac{k+n+1}{2}}} \left(\frac{\gamma_{th}}{\varphi}\right)^{m+\frac{k-n+1}{2}} \times K_{k-n+1}\left(2\sqrt{\frac{b_1 b_2 \gamma_{th}}{\kappa\varphi}}\right), \\ P_{out\_B} &= 1 - 2a_1a_2 \times e^{-\frac{b_1\gamma_{th}}{\varphi}} \sum_{l=0}^{\infty}\sum_{k=0}^{\infty}\sum_{m=0}^{l}\sum_{n=0}^{m} \frac{K^{l+k} b_2^{\frac{k+n-1}{2}} b_1^{\frac{2m+k-n-1}{2}}}{l!n!(m-n)!(k!)^2 \kappa^{\frac{k+n+1}{2}}} \left(\frac{\gamma_{th}}{\varphi}\right)^{m+\frac{k-n+1}{2}} \times K_{k-n+1}\left(2\sqrt{\frac{b_1 b_2 \gamma_{th}}{\kappa\varphi}}\right), \end{aligned} \tag{10}$$

where $K_v(\bullet)$ *is the modified Bessel function of the second kind and vth order.*

Proof. See Appendix A.

3.2. Achievable throughput

The achievable throughput at the source nodes A and B can be computed by:

$$\tau_j = (1 - P_{out\_j}) \times R \times (1 - \alpha), \tag{11}$$

where $j \in (A, B)$.

3.3. Symbol error ratio analysis

In this section, the expressions for the SER at the nodes A and B of the proposed system are obtained. Thus, we have SER equations as (12) and (13) below [14].

$$SER_j = E\left[\varpi Q(\sqrt{2\theta\gamma_j})\right], \tag{12}$$

where $j \in (A, B)$, $Q(t) = \frac{1}{\sqrt{2\pi}} \int_t^{\infty} e^{-x^2/2} dx$ is the Gaussian Q-function and ϖ and θ are constants specific for the modulation type. Here (ϖ, θ) = (1, 1) for binary phase-shift keying (BPSK) and (ϖ, θ) = (1, 2) for quadrature phase shift keying (QPSK).

As a result, before obtaining the SER performance, the distribution function of γ_j is expected. Then, we begin rewriting the SER expression given in (12) directly regarding the outage probability at the source by using integration, as follows:

$$SER_j = \frac{\varpi\sqrt{\theta}}{2\sqrt{\pi}} \int_0^{\infty} \frac{e^{-\theta x}}{\sqrt{x}} F_{\gamma_j}(x) dx. \tag{13}$$

Theorem 2. *The SER at the nodes A and B of the proposed system can be calculated as follows:*

$$SER_A = \frac{\varpi}{2} - \frac{a_1 a_2 \varpi \sqrt{\theta}}{2\sqrt{\pi}} \times \sum_{l=0}^{\infty}\sum_{k=0}^{\infty}\sum_{m=0}^{l}\sum_{n=0}^{m} \frac{K^{l+k} b_1^{\frac{k+n-2}{2}} b_2^{\frac{2m+k-n-2}{2}}}{l!n!(m-n)!(k!)^2 \kappa^{\frac{k+n}{2}} \varphi^{m+\frac{k-n}{2}}} \times \left[\frac{b_2}{\varphi} + \theta\right]^{-\left(\frac{2m-n+k+1}{2}\right)}$$
$$\times \Gamma\left(m+\frac{1}{2}\right) \times \Gamma\left(m-n+k+\frac{3}{2}\right) \times \exp\left[\frac{b_1 b_2}{2\kappa b_2 + 2\kappa\theta\varphi}\right] \times W_{-\frac{2m-n+k+1}{2}, \frac{k-n+1}{2}}\left[\frac{b_1 b_2}{\kappa\{b_2 + \theta\varphi\}}\right], \quad (14)$$

$$SER_B = \frac{\varpi}{2} - \frac{a_1 a_2 \varpi \sqrt{\theta}}{2\sqrt{\pi}} \times \sum_{l=0}^{\infty}\sum_{k=0}^{\infty}\sum_{m=0}^{l}\sum_{n=0}^{m} \frac{K^{l+k} b_2^{\frac{k+n-2}{2}} b_1^{\frac{2m+k-n-2}{2}}}{l!n!(m-n)!(k!)^2 \kappa^{\frac{k+n}{2}} \varphi^{m+\frac{k-n}{2}}} \times \left[\frac{b_1}{\varphi} + \theta\right]^{-\left(\frac{2m-n+k+1}{2}\right)}$$
$$\times \Gamma\left(m+\frac{1}{2}\right) \times \Gamma\left(m-n+k+\frac{3}{2}\right) \times \exp\left[\frac{b_1 b_2}{2\kappa b_1 + 2\kappa\theta\varphi}\right] \times W_{-\frac{2m-n+k+1}{2}, \frac{k-n+1}{2}}\left[\frac{b_1 b_2}{\kappa\{b_1 + \theta\varphi\}}\right]. \quad (15)$$

Proof. See Appendix B.

3.4. Optimal time-switching factor

The optimal value α^* can be obtained by solving the equation $\frac{d\tau_j(\alpha)}{d\alpha} = 0$. Given the achievable throughput expression in (10) and (11), this optimization problem does not admit a closed-form solution. However, the optimal α^* can be efficiently solved via numerical calculation, as illustrated below.

Here we can use the Golden section search algorithm to find the optimal factor α^*. This algorithm has been used in many global optimization problems in communications, for example in [15]. The detailed algorithm, as well as the related theory, is described in [16,17].

4. NUMERICAL RESULTS AND DISCUSSION

In this section, we investigate the system performance (in terms of the throughput, outage probability, optimal time switching factor, and SER) of the energy harvesting based TWFD relaying network over a Rician fading environment by using Monte Carlo simulation [16,17]. The simulation parameters are listed in Table 1.

The influence of the Rician K-factor K on the outage probability and throughput of the model system is shown in Fig. 3a and 3b, respectively. In this simulation process, the main parameters of the proposed system are set as $\alpha = 0.5$; $P_{AB}/N_0 = 20$ dB; $\Omega = 0,\ 0.5,\ 5,\ 15$. Figure 3 demonstrates that the outage probability

Table 1. Simulation parameters

Name	Symbol	Value
Energy harvesting efficiency	η	0.7
Mean $\lvert h_{AR} \rvert^2$	λ_1	0.5
Mean $\lvert h_{BR} \rvert^2$	λ_2	0.5
Rician K-factor	K	3
SNR threshold	γ_{th}	7
Source power to noise ratio	P_{AB}/N_0	0–30 dB
Residual self-interference	$\Omega_{AA} = \Omega_{BB} = \Omega_{RR} = \Omega$	0–15 dB
Source rate	R	1.5 (bit/s)/Hz

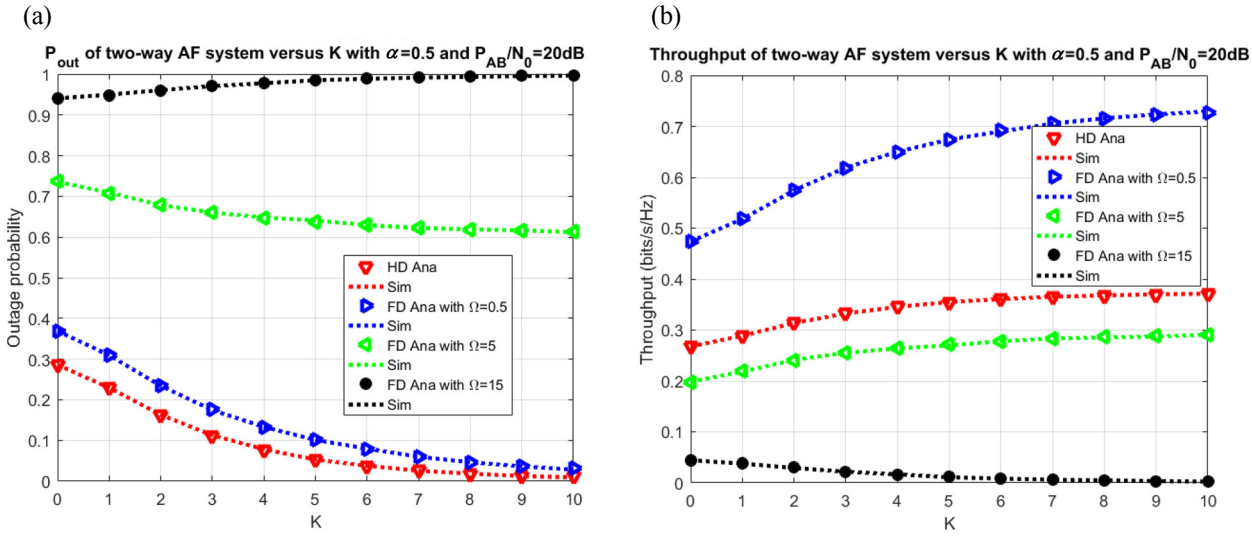

Fig. 3. Outage probability (a) and the achievable throughput (b) of the system model versus the Rician K-factor K.

decreased and the throughput increased crucially while K increased from 0 to 10. Moreover, the analytical results agree well with the Monte Carlo simulation results, validating the theoretical derivations.

The influence of residual self-interference Ω on the outage probability and the achievable throughput of the model system is illustrated in Fig. 4a and 4b. Here, α is set at 0.5, 0.1, 0.9 and the ratio P_{AB}/N_0 at 20 dB. From the simulation, it is clear that the achievable throughput increases and the outage probability decreases significantly while Ω increases from 0 to 15. In these cases, the figures reveal that the simulation results match tightly with analytical expressions in Section 3.

Moreover, Fig. 5a and 5b present the effect of the ratio P_{AB}/N_0 on the outage probability and the achievable throughput with Ω = 0, 0.5, 5, 15 and α = 0.5 for the proposed system. The results show that the achievable throughput increased and the outage probability decreased significantly when the ratio P_{AB}/N_0 increased from 0 to 30 dB. In Fig. 5, all the analytical and simulation results agreed well with each other.

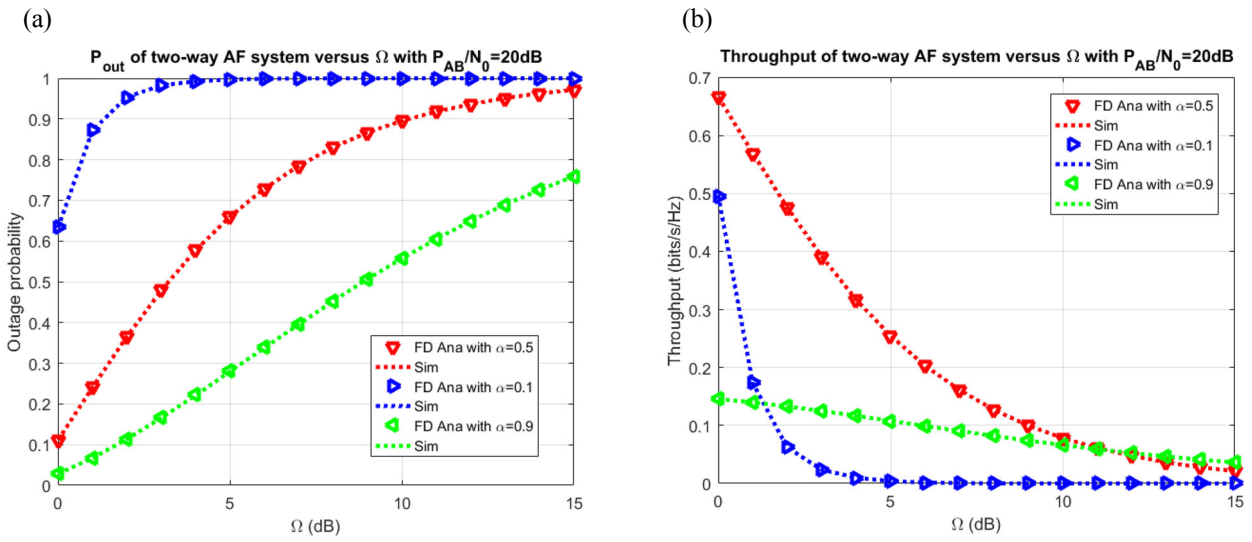

Fig. 4. Outage probability (a) and the achievable throughput (b) of the system model versus residual self-interference Ω.

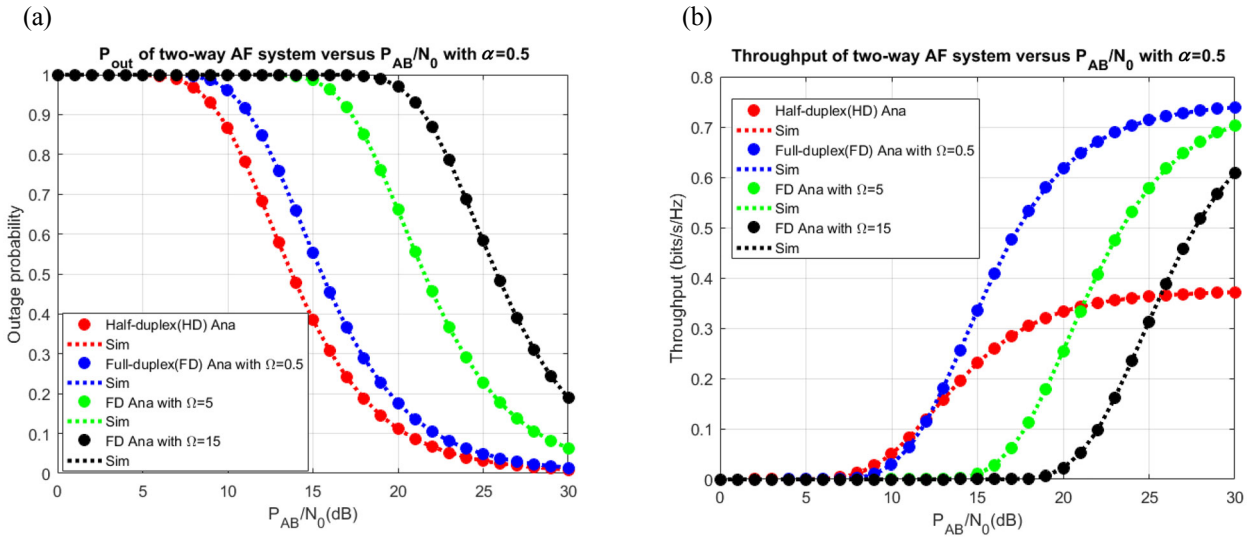

Fig. 5. Outage probability (a) and the achievable throughput (b) of the system model versus the ratio P_{AB}/N_0.

The influence of the source rate R on the outage probability and the achievable throughput of the system model with $P_{AB}/N_0 = 20$ dB and $\Omega = 0,\ 0.5,\ 5,\ 15$ is illustrated in Fig. 6a and 6b, respectively. Figure 6a shows that the outage probability increased crucially with increasing the rate R. However, the system throughput only increased in the interval of R from 0 to the optimal value around 2. After that, it significantly fell to 0 at the rate around 4. In particular, the simulation lines wholly match with the analytical lines in all the above figures.

Finally, the optimal time switching factor versus the ratio P_{AB}/N_0 is illustrated in Fig. 7. Figure 8 shows the SER of the proposed system versus P_{AB}/N_0. In these figures, the simulation results match tightly with the analytical results in Section 3.

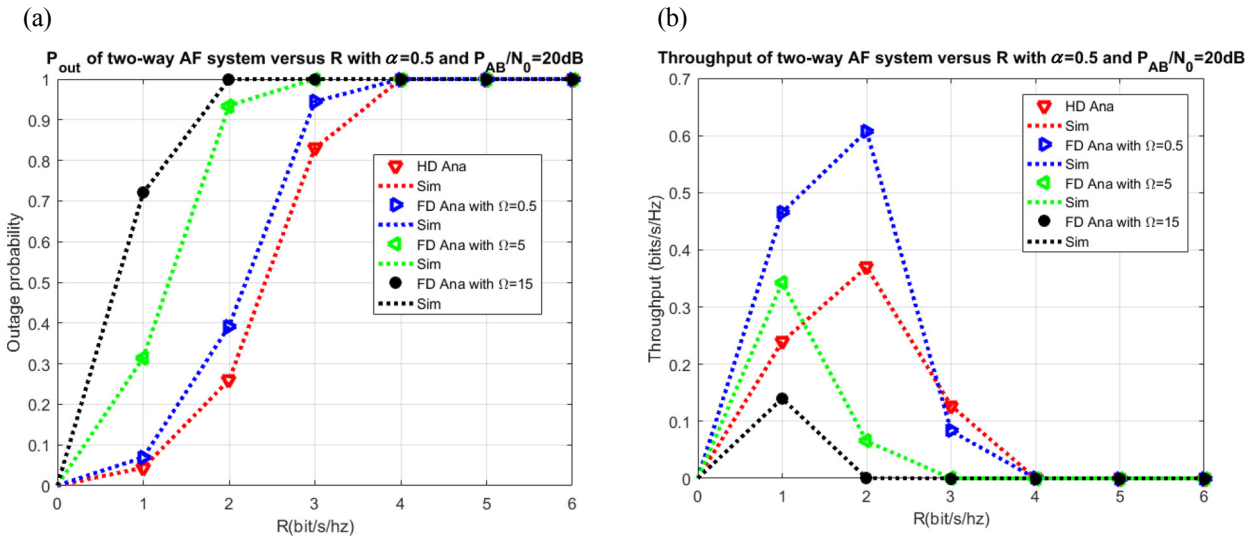

Fig. 6. Outage probability (a) and the achievable throughput (b) of the system throughput versus the source rate R.

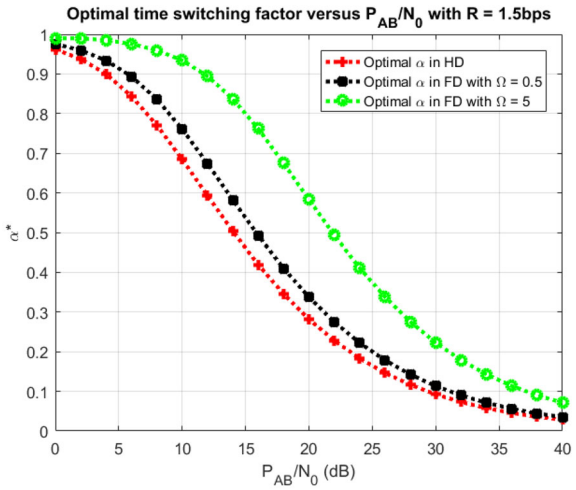

Fig. 7. Optimal time switching factor versus the ratio P_{AB}/N_0.

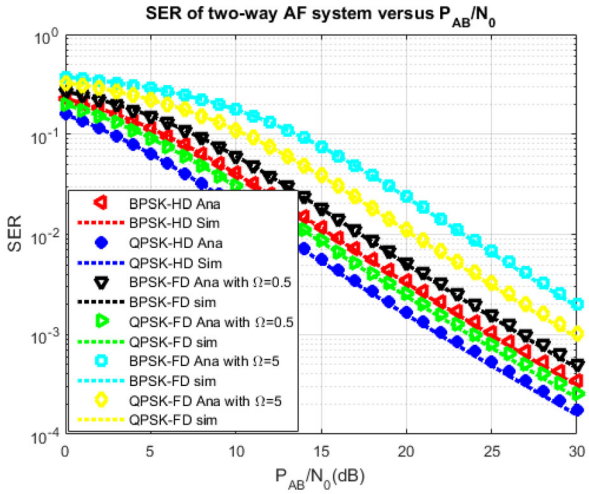

Fig. 8. Symbol error ratio versus P_{AB}/N_0.

5. CONCLUSIONS

In this paper, the system performance of the energy harvesting based two-way full-duplex relaying network over a Rician fading environment is proposed and investigated. In order to analyse the system performance at the destination node, analytical expressions for the outage probability, throughput, optimal time switching factor, and system error ratio are proposed and investigated. The research results show that the analytical mathematical expression and the simulation results using the Monte Carlo method totally matched each other. Moreover, this paper provides practical insights into the effect of various system parameters on the system performance. The results could provide a prospective solution for the communication network via a helping relay.

APPENDIX A

PROOF OF THEOREM 1

At first, we need to determine the probability density function (PDF) and the cumulative density function (CDF) of a random variable (RV) ω_i whose $i \in \{1,2\}$.

In [18] the PDF of the RV can be formulated by the following formula:

$$f_{\omega_i}(x) = \frac{(K+1)e^{-K}}{\lambda_i} e^{-\frac{(K+1)x}{\lambda_i}} I_0\left(2\sqrt{\frac{K(K+1)x}{\lambda_i}}\right), \tag{A1}$$

where λ_i is the mean value of RV ω_i, K is the Rician K-factor defined as the ratio of the power of the line-of-sight (LOS) component to the scattered components, and $I_0(\bullet)$ is the zeroth order modified Bessel function of the first kind.

Now, with using $a_i = \frac{(K+1)e^{-K}}{\lambda_i}$, $b_i = \frac{K+1}{\lambda_i}$ and $I_0(x) = \sum_{l=0}^{\infty} \frac{x^{2l}}{2^{2l}(l!)^2}$ [19], equation (A1) can be rewritten as :

$$f_{\omega_i}(x) = a_i \sum_{l=0}^{\infty} \frac{(b_i K)^l}{(l!)^2} x^l e^{-b_i x}. \tag{A2}$$

The CDF of the RV ω_i can be obtained like in [20, 21]. We have the following:

$$F_{\omega_i}(\varsigma)=\int_0^{\varsigma} f_{\omega_i}(x)dx=1-\frac{a_i}{b_i}\sum_{l=0}^{\infty}\sum_{m=0}^{l}\frac{K^l b_i^m}{l!m!}\varsigma^m e^{-b_i\varsigma}. \tag{A3}$$

Then the outage probability at the node A can be calculated as:

$$P_{out\_A}=F_{\gamma_A}(\gamma_{th})=\Pr\left(\gamma_A<\gamma_{th}\right)=\Pr\left(\frac{\kappa\varphi\omega_1\omega_2}{\kappa\omega_1+1}<\gamma_{th}\right). \tag{A4}$$

Here $\gamma_{th}=2^{2R}-1$.

Now (A4) can reformulated as:

$$P_{out\_A}=\int_0^{\infty}\Pr\left\{\omega_2<\frac{\gamma_{th}\kappa\omega_1+\gamma_{th}}{\kappa\varphi\omega_1}\mid\omega_1\right\}f_{\omega_1}(\omega_1)d\omega_1=\int_0^{\infty}F_{\omega_2}\left\{\omega_2<\frac{\gamma_{th}\kappa\omega_1+\gamma_{th}}{\kappa\varphi\omega_1}\mid\omega_1\right\}f_{\omega_1}(\omega_1)d\omega_1. \tag{A5}$$

By combining (19) with (16) and (17), we have:

$$P_{out\_A}=1-\int_0^{\infty}\frac{a_2}{b_2}\sum_{l=0}^{\infty}\sum_{m=0}^{l}\frac{K^l {b_2}^m}{l!m!}\left[\frac{\kappa\omega_1\gamma_{th}+\gamma_{th}}{\kappa\varphi\omega_1}\right]^m\times e^{-b_2\left[\frac{\kappa\omega_1\gamma_{th}+\gamma_{th}}{\kappa\varphi\omega_1}\right]}\times a_1\sum_{l=0}^{\infty}\frac{(b_1K)^l}{(l!)^2}\omega_1^l e^{-b_1\omega_1}d\omega_1, \tag{A6}$$

$$P_{out\_A}=1-\int_0^{\infty}a_1a_2\sum_{l=0}^{\infty}\sum_{k=0}^{\infty}\sum_{m=0}^{l}\frac{K^{l+k}b_2^{m-1}b_1^k}{l!m!(k!)^2}\left(\frac{\gamma_{th}}{\varphi}\right)^m\left[1+\frac{1}{\kappa\omega_1}\right]^m\times e^{-\frac{b_2\gamma_{th}}{\varphi}}\times e^{-\frac{b_2\gamma_{th}}{\kappa\varphi\omega_1}}\times\omega_1^k e^{-b_1\omega_1}d\omega_1. \tag{A7}$$

Now by applying the equation $(x+y)^m=\sum_{n=0}^{m}\binom{m}{n}x^{m-n}y^n$ to (A7), the outage probability can demonstrated as follows:

$$P_{out\_A}=1-\int_0^{\infty}a_1a_2\sum_{l=0}^{\infty}\sum_{k=0}^{\infty}\sum_{m=0}^{l}\frac{K^{l+k}b_1^k b_2^{m-1}}{l!m!(k!)^2}\left(\frac{\gamma_{th}}{\varphi}\right)^m\sum_{n=0}^{m}\binom{m}{n}\left[\frac{1}{\kappa\omega_1}\right]^n\times e^{-\frac{b_2\gamma_{th}}{\varphi}}\times e^{-\frac{b_2\gamma_{th}}{\kappa\varphi\omega_1}}\times\omega_1^k\times e^{-b_1\omega_1}d\omega_1, \tag{A8}$$

$$P_{out\_A}=1-a_1a_2\times e^{-\frac{b_2\gamma_{th}}{\varphi}}\sum_{l=0}^{\infty}\sum_{k=0}^{\infty}\sum_{m=0}^{l}\sum_{n=0}^{m}\frac{K^{l+k}b_1^k b_2^{m-1}}{l!n!(m-n)!(k!)^2\kappa^n}\left(\frac{\gamma_{th}}{\varphi}\right)^m\times\int_0^{\infty}\omega_1^{k-n}\times e^{-\frac{b_2\gamma_{th}}{\kappa\varphi\omega_1}}\times e^{-b_1\omega_1}d\omega_1. \tag{A9}$$

Using Eq. [3.471,9] in the Table of Integrals [19], equation (A9) can be reformulated as follows:

$$P_{out\_A}=1-2a_1a_2\times e^{-\frac{b_2\gamma_{th}}{\varphi}}\sum_{l=0}^{\infty}\sum_{k=0}^{\infty}\sum_{m=0}^{l}\sum_{n=0}^{m}\frac{K^{l+k}b_1^k b_2^{m-1}}{l!n!(m-n)!(k!)^2\kappa^n}\left(\frac{\gamma_{th}}{\varphi}\right)^m\times\left(\frac{b_2\gamma_{th}}{b_1\kappa\varphi}\right)^{\frac{k-n+1}{2}}\times K_{k-n+1}\left(2\sqrt{\frac{b_2b_1\gamma_{th}}{\kappa\varphi}}\right), \tag{A10}$$

$$P_{out\_A}=1-2a_1a_2\times e^{-\frac{b_2\gamma_{th}}{\varphi}}\sum_{l=0}^{\infty}\sum_{k=0}^{\infty}\sum_{m=0}^{l}\sum_{n=0}^{m}\frac{K^{l+k}b_1^{\frac{k+n-1}{2}}b_2^{\frac{2m+k-n-1}{2}}}{l!n!(m-n)!(k!)^2\kappa^{\frac{k+n+1}{2}}}\left(\frac{\gamma_{th}}{\varphi}\right)^{m+\frac{k-n+1}{2}}\times K_{k-n+1}\left(2\sqrt{\frac{b_1b_2\gamma_{th}}{\kappa\varphi}}\right). \tag{A11}$$

The proof for the outage probability at the node B is similar:

$$P_{out\_B} = 1 - 2a_1a_2 \times e^{-\frac{b_1\gamma_{th}}{\varphi}} \sum_{l=0}^{\infty}\sum_{k=0}^{\infty}\sum_{m=0}^{l}\sum_{n=0}^{m} \frac{K^{l+k} b_2^{\frac{k+n-1}{2}} b_1^{\frac{2m+k-n-1}{2}}}{l!n!(m-n)!(k!)^2 \kappa^{\frac{k+n+1}{2}}} \left(\frac{\gamma_{th}}{\varphi}\right)^{m+\frac{k-n+1}{2}} \times K_{k-n+1}\left(2\sqrt{\frac{b_1 b_2 \gamma_{th}}{\kappa\varphi}}\right). \quad \text{(A12)}$$

□

APPENDIX B

PROOF OF THEOREM 1

From (13), we have:

$$SER_A = \frac{\varpi\sqrt{\theta}}{2\sqrt{\pi}} \int_0^{\infty} \frac{e^{-\theta x}}{\sqrt{x}} \left(1 - 2a_1a_2 \times e^{-\frac{b_2 x}{\varphi}} \sum_{l=0}^{\infty}\sum_{k=0}^{\infty}\sum_{m=0}^{l}\sum_{n=0}^{m} \frac{K^{l+k} b_1^{\frac{k+n-1}{2}} b_2^{\frac{2m+k-n-1}{2}}}{l!n!(m-n)!(k!)^2 \kappa^{\frac{k+n+1}{2}}} \times \left(\frac{x}{\varphi}\right)^{m+\frac{k-n+1}{2}} \times K_{k-n+1}\left(2\sqrt{\frac{b_1 b_2 x}{\kappa\varphi}}\right)\right) dx, \quad \text{(B1)}$$

$$SER_A = \frac{\varpi\sqrt{\theta}}{2\sqrt{\pi}} \int_0^{\infty} \frac{e^{-\theta x}}{\sqrt{x}} dx - \frac{a_1 a_2 \varpi\sqrt{\theta}}{\sqrt{\pi}} \int_0^{\infty} \left\{ \sum_{l=0}^{\infty}\sum_{k=0}^{\infty}\sum_{m=0}^{l}\sum_{n=0}^{m} \frac{K^{l+k} b_1^{\frac{k+n-1}{2}} b_2^{\frac{2m+k-n-1}{2}}}{l!n!(m-n)!(k!)^2 \kappa^{\frac{k+n+1}{2}} \varphi^{m+\frac{k-n+1}{2}}} \times x^{\frac{2m-n+k}{2}} \times e^{-x\left[\frac{b_2}{\varphi}+\theta\right]} \times K_{k-n+1}\left(2\sqrt{\frac{b_1 b_2 x}{\kappa\varphi}}\right) \right\} dx. \quad \text{(B2)}$$

In these equations, we denote

$$J_1 = \frac{\varpi\sqrt{\theta}}{2\sqrt{\pi}} \int_0^{\infty} \frac{e^{-\theta x}}{\sqrt{x}} dx, \quad \text{(B3)}$$

$$J_2 = \int_0^{\infty} x^{\frac{2m-n+k}{2}} \times e^{-x\left[\frac{b}{\varphi}+\theta\right]} \times K_{k-n+1}\left(2b\sqrt{\frac{x}{\kappa\varphi}}\right) dx. \quad \text{(B4)}$$

Using equation (3.361,1) from [19], we have:

$$J_1 = \frac{\varpi\sqrt{\theta}}{2\sqrt{\pi}} \times \frac{\sqrt{\pi}}{\sqrt{\theta}} = \frac{\varpi}{2}. \quad \text{(B5)}$$

By using equation (6.643,3) from [19], we have:

$$\int_0^{\infty} t^{\mu-\frac{1}{2}} e^{-\alpha t} K_{2v}(2\beta\sqrt{t}) dt = \frac{\alpha^{-\mu}}{2\beta} \Gamma\left(\mu - v + \frac{1}{2}\right) \Gamma\left(\mu + v + \frac{1}{2}\right) \exp\left(\frac{\beta^2}{2\alpha}\right) W_{-\mu,v}\left(\frac{\beta^2}{\alpha}\right), \quad \text{(B6)}$$

where $\Gamma(\bullet)$ is the gamma function and $W(\bullet)$ is the Whittaker function.

Finally, we can reformulate (B4) to the following:

$$J_2 = \left[\frac{b}{\varphi}+\theta\right]^{-\frac{2m-n+k+1}{2}} \times \frac{\sqrt{\kappa\varphi}}{2b} \times \Gamma\left(m+\frac{1}{2}\right) \times \Gamma\left(m-n+k+\frac{3}{2}\right) \times \exp\left[\frac{b^2}{2\kappa b+2\kappa\theta\varphi}\right] \times W_{-\frac{2m-n+k+1}{2},\frac{k-n+1}{2}}\left[\frac{b^2}{\kappa\{b+\theta\varphi\}}\right], \quad \text{(B7)}$$

$$SER_A = \frac{\varpi}{2} - \frac{a^2\varpi\sqrt{\theta}}{\sqrt{\pi}} \times \sum_{l=0}^{\infty}\sum_{k=0}^{\infty}\sum_{m=0}^{l}\sum_{n=0}^{m} \frac{K^{l+k}b^{m+k-1}}{l!n!(m-n)!(k!)^2\kappa^{\frac{k+n+1}{2}}\varphi^{m+\frac{k-n+1}{2}}} \times \left[\frac{b}{\varphi}+\theta\right]^{-\frac{2m-n+k+1}{2}} \times \frac{\sqrt{\kappa\varphi}}{2b} \times \Gamma\left(m+\frac{1}{2}\right) \times \Gamma\left(m-n+k+\frac{3}{2}\right) \times \exp\left[\frac{b^2}{2\kappa b+2\kappa\theta\varphi}\right] \times W_{-\frac{2m-n+k+1}{2},\frac{k-n+1}{2}}\left[\frac{b^2}{\kappa\{b+\theta\varphi\}}\right]. \quad \text{(B8)}$$

From (B7) we can have formula (14).
In the same way as node A, the SER of the node B can be demonstrated as formula (15). □

ACKNOWLEDGEMENTS

This work was supported by the grant SGS, registration No. SP2018/59, conducted at VSB Technical University of Ostrava, Czech Republic, and partly by The Ministry of Education, Youth and Sports from the Large Infrastructures for Research, Experimental Development, and Innovations project, registration No. LM2015070. The publication costs of this article were partially covered by the Estonian Academy of Sciences.

REFERENCES

1. Bi, S., Ho, C. K., and Zhang, R. Wireless powered communication: opportunities and challenges. *IEEE Commun. Mag.*, 2015, **53**(4), 117–125.
2. Niyato, D., Kim, D. I., Maso, M., and Han, Z. Wireless powered communication networks: research directions and technological approaches. *IEEE Wireless Commun.*, 2017, **24**(6), 2–11.
3. Yu, H., Lee, H., and Jeon, H. What is 5G? Emerging 5G mobile services and network requirements. *Sustainability*, 2017, **9**, 1848.
4. Duarte, M., Dick, C., and Sabharwal, A. Experiment-driven characterization of full-duplex wireless systems. *IEEE Trans. Wireless Commun.*, 2012, **12**, 4296–4307.
5. Lee, W. C. Y. The most spectrum-efficient duplexing system: CDD. *IEEE Commun. Mag.*, 2012, **40**, 163–166.
6. Wang, C-X., Haider, F., Gao, X., You, X-H., Yang, Y., Yuan, D., et al. Cellular architecture and key technologies for 5G wireless communication networks. *IEEE Commun. Mag.*, 2014, **52**, 122–130.
7. Ju, H., Oh, E., and Hong, D. Catching resource-devouring worms in next-generation wireless relay systems: two-way relay and full-duplex relay. *IEEE Commun. Mag.*, 2009, **47**, 58–65.
8. Riihonen, T., Werner, S., Wichman, R., and Hämäläinen, J. Outage probabilities in infrastructure-based single-frequency relay links. In *Proceedings of IEEE Wireless Communications and Networking Conference*. IEEE, 2009.
9. Ng, D. W. K., Lo, E. S., and Schober, R. Dynamic resource allocation in MIMO-OFDMA systems with full duplex and hybrid relaying. *IEEE Trans. Commun.*, 2012, **60**, 1291–1304.
10. Krikidis, I., Suraweera, H. A., Smith, P. J., and Yuen, C. Full-duplex relay selection for amplify-and-forward cooperative networks. *IEEE Trans. Wireless Commun.*, 2012, **11**, 4381–4393.
11. Valenta, C. R. and Durgin, G. D. Harvesting wireless power: survey of energy-harvester conversion efficiency in far-field, wireless power transfer systems. *IEEE Microwave Mag.*, 2014, **15**(4), 108–120.
12. Louie, R., Li, Y., and Vucetic, B. Practical physical layer network coding for two-way relay channels: performance analysis and comparison. *IEEE Trans. Wireless Commun.*, 2010, **9**, 764–777.
13. Riihonen, T., Werner, S., and Wichman, R. Hybrid full-duplex/half-duplex relaying with transmit power adaptation. *IEEE Trans. Wireless Commun.*, 2011, **10**, 3074–3085.

14. Duong, T. Q., Duy, T. T., Matthaiou, M., Tsiftsis, T., and Karagiannidis, G. K. Cognitive cooperative networks in dual-hop asymmetric fading channels. In *IEEE Global Communications Conference (GLOBECOM)*. Conference paper, 2013.
15. Chong, E. K. and Zak, S. H. *An Introduction to Optimization*. John Wiley & Sons, 2013.
16. Nguyen, T. N., Minh, T. H. Q., Tran, P. T., and Voznak, M. Energy harvesting over Rician fading channel: a performance analysis for half-duplex bidirectional sensor networks under hardware impairments. *Sensors*, 2018, **18**(6), 1781.
17. Nguyen, T. N., Minh, T. H. Q., Tran, P. T., and Voznak, M. Adaptive energy harvesting relaying protocol for two-way half duplex system network over Rician fading channel. *Wireless Commun. Mobile Comput.*, **2018**, Article ID 7693016.
18. Suraweera, H., Karagiannidis, G., and Smith, P. Performance analysis of the dual-hop asymmetric fading channel. *IEEE Trans. Wireless Commun.*, 2009, **8**, 2783–2788.
19. Zwillinger, D. (ed.). *Table of Integrals, Series, and Products.* Elsevier, 2015.
20. Bhatnagar, M. R. On the capacity of decode-and-forward relaying over Rician fading channels. *IEEE Commun. Lett.*, 2013, **17**, 1100–1103.
21. Nguyen, T. N., Minh, T. H. Q., Tran, P. T., Voznak, M., Duy, T. T., Nguyen, T-L., and Tin, P. T. Performance enhancement for energy harvesting based two-way relay protocols in wireless ad-hoc networks with partial and full relay selection methods. *Ad Hoc Networks*, **84**, 178–187.

Energia kogumine kahekanalilises täisduplekstranslatsioonivõrgus, kasutades Rice'i kustumismeediumi: efektiivsuse analüüs

Tan N. Nguyen, Minh Tran, Duy-Hung Ha, Thanh-Long Nguyen ja Miroslav Voznak

Täisdupleksülekanne on kommunikatsioonisüsteemide läbilaskevõime suurendamiseks paljulubav tehnika. Artiklis on esitatud ja uuritud süsteemi suutlikkust energia kogumisel, mis baseerub kahekanalilisel täisduplekstranslatsioonivõrgul, kasutades Rice'i kustumismeediumi.

Esimeses etapis on analüüsitud analüütilisi valemeid ja need on ära toodud esitatud süsteemi läbilaskevõime, jõudeaja tõenäosuse, optimaalse ajalise lülitusfaktori ning sümbolite veasuhte (SER) arvutamiseks.

Teises etapis on esitatud süsteemi suutlikkuse erinevate parameetrite mõju ja nende uuring. Lõppetapis on esitatud analüütiliste tulemuste analüüs Monte Carlo simulatsioonimeetodil. Numbrilised tulemused, mis näitavad ja kinnitavad analüütilisi ning simulatsiooni tulemusi, on omavahel täielikus vastavuses.